Title
Comparing Discretized Beam Arrays to Ideal LG0,1 Beams in Integrated Structured-Light Setups

Permalink

Author
Castrejon, Gustavo

Publication Date
2025-12-18

Comparing Discretized Beam Arrays to Ideal $LG_{0,1}$ Beams in Integrated Structured-Light Setups

Gustavo Castrejon
Department of Electrical and Computer Engineering
University of California, Los Angeles, CA 90095, USA
castrejongus@ucla.edu

Abstract

In this review, I model a simple seven-site hexagonal beam array inspired by Lemons et al. [1] and compare its output to an ideal $LG_{0,1}$ (donut-shaped) beam. I use basic similarity metrics in the far field (including an MSE and an overlap score) to gauge how close the array comes to the ideal case. The main mismatch shows up as a slight ripple around the ring and small sidelobes, which is expected when a smooth phase pattern is built from only a few beamlets.

Introduction

Structured light refers to laser beams that are intentionally shaped so their intensity, phase, or polarization vary in space, instead of looking like the fundamental Gaussian beam profile. One well-known example is a Laguerre–Gaussian (LG) beam, which has a donut-shaped intensity profile and a twisting phase pattern that gives the beam orbital angular momentum (OAM). These kinds of beams are useful in areas like free-space communication, imaging, and optical manipulation because they offer extra "degrees of freedom" that can be engineered for specific tasks [3].

Lemons et al. [1] present an alternative approach to generating these structured beams. Instead of shaping one laser beam with a spatial light modulator, they split the light into multiple smaller beams and control each one's phase, amplitude, polarization, and timing. A microlens array then brings all of these beamlets back together to create a single structured output. With this approach, they show that even a small number of beams can produce patterns similar to OAM beams and other complex light structures.

However, using only a few beams also leads to discretization when trying to recreate a smooth ideal beam using a limited number of samples. This raises an important question: how close can a seven-site hexagonal array come to an ideal $LG_{0,1}$ beam, and what kind of errors appear because of the limited number of channels?

Motivated by this architecture, I focus on numerically quantifying how channel discretization affects the fidelity of an OAM-like donut beam. In particular, this work studies the seven-site geometry introduced in [1] and evaluates how closely it can reproduce an ideal $LG_{0,1}$ mode when only a small number of phase-controlled beamlets are available.

Here, I summarize the main ideas behind the Lemons et al. architecture and use standard Gaussian and Laguerre–Gaussian beam theory [2] to model a simple phased array that imitates an $LG_{0,1}$ beam. I compare the simulated array to the ideal mode, calculate the error between them, and discuss what this tells us about the limits and potential of discretized structured-light generation.

Beyond being a modeling exercise, discretization fidelity matters in practical systems. In free-space optical communication, reduced mode purity can translate into coupling loss and lower link margin when using mode-division multiplexing or OAM-based channels. In optical manipulation and precision metrology, sidelobes and azimuthal modulation can introduce unintended trapping sites or background signals that degrade controllability. For integrated photonics, quantifying the channel-count-versus-fidelity trade-off helps determine how many phase-controlled emitters are required to achieve a target structured-beam quality within area and power constraints.

Methods

To represent the ideal donut-shaped OAM beam, I use the standard Laguerre–Gaussian mode with radial index $p = 0$ and azimuthal index $\ell = 1$. This mode, written as $\mathrm{LG}_{0,1}$, has a single ring of intensity and a phase that wraps once around 2π, creating the characteristic on-axis null.

The LG mode expression used below and the Fourier (Fraunhofer) far-field relationship used for propagation follow standard Gaussian/LG beam and Fourier-optics treatments (Liu [2]).

At the beam waist $z = 0$, the electric-field envelope in cylindrical coordinates (r, θ) can be written as

$$E_{\mathrm{LG}_{0,1}}(r, \theta) = C \left(\frac{\sqrt{2}\, r}{w_0} \right) \exp\left(-\frac{r^2}{w_0^2} \right) \exp(i\theta), \tag{1}$$

where w_0 is the beam waist and C is a normalization constant chosen so that the total power is unity. Cartesian and cylindrical coordinates are related by $x = r\cos\theta$ and $y = r\sin\theta$.

For $\ell = 1$, this expression produces the expected donut intensity profile

$$I_{\mathrm{LG}_{0,1}}(r, \theta) = \left| E_{\mathrm{LG}_{0,1}}(r, \theta) \right|^2. \tag{2}$$

This $\mathrm{LG}_{0,1}$ mode serves as the "ground truth" beam that the discretized phased array will be compared against.

To imitate the structured-light architecture used in [1], I model a simple hexagonal array of seven Gaussian beamlets. We consider a seven-site hexagonal geometry; the center site is present but disabled ($A_{\mathrm{center}} = 0$), so synthesis uses the six outer beamlets. One beamlet is placed at the center, and the remaining six are arranged on a ring at radius R. Their angular positions are

$$\theta_k = \frac{2\pi(k-1)}{6}, \qquad k = 1, \ldots, 6. \tag{3}$$

Each beamlet is treated as a fundamental Gaussian with waist w_b. The field from the k-th outer beamlet is

$$E_k(x, y) = A_k \exp\left[-\frac{(x - x_k)^2 + (y - y_k)^2}{w_b^2} \right] \exp(i\phi_k), \tag{4}$$

where $(x_k, y_k) = (R\cos\theta_k, R\sin\theta_k)$ are the beamlet centers.

To approximate an $\ell = 1$ OAM mode, I set all outer-ring amplitudes equal ($A_k = 1$) and impose a 2π phase ramp around the ring:

$$\phi_k = \theta_k, \qquad k = 1, \ldots, 6. \tag{5}$$

In the simulations reported here, the central beamlet is suppressed ($A_{\mathrm{center}} = 0$) to preserve the on-axis null.

The total near-field array is then

$$E_{\text{array}}(x,y) = \sum_{k=1}^{6} E_k(x,y), \tag{6}$$

and the corresponding intensity is

$$I_{\text{array}}(x,y) = \left|E_{\text{array}}(x,y)\right|^2. \tag{7}$$

All calculations are performed on a uniform $N \times N$ 2D Cartesian grid in MATLAB (e.g., $N = 512$). I evaluate both the ideal $\text{LG}_{0,1}$ field and the array field on the same grid.

To approximate the far field, I use the Fraunhofer (Fourier-transform) relationship between the field at the waist and the far-field angular spectrum:

$$\tilde{E}(k_x,k_y) = \mathcal{F}\{E(x,y)\}. \tag{8}$$

The normalized far-field intensity is computed as

$$I_{\text{far}}(k_x,k_y) = \frac{\left|\tilde{E}(k_x,k_y)\right|^2}{\sum_{k_x,k_y}\left|\tilde{E}(k_x,k_y)\right|^2}. \tag{9}$$

To measure how closely the array matches the ideal beam, I compute the mean-squared error (MSE) between the normalized intensities of the two beams:

$$\text{MSE} = \frac{1}{M}\sum_{j=1}^{M}\left(I_{\text{array},j} - I_{\text{LG},j}\right)^2, \tag{10}$$

where M is the number of grid points (pixels) in the 2D far-field intensity map.

All calculations are performed on a uniform $N \times N$ Cartesian grid in MATLAB (e.g., $N = 512$) over a square window of side length $L = 4$ mm. For the results reported here, I choose an ideal LG beam waist of $w_0 = 0.6$ mm, a beamlet waist of $w_b = 0.5$ mm, and a hexagonal ring radius of $R = 0.8$ mm.

Results and Interpretation

Figure 1 shows the normalized far-field intensity of the ideal $\text{LG}_{0,1}$ mode. As expected for $\ell = 1$, the pattern exhibits a pronounced on-axis null and a single dominant annular maximum with minimal azimuthal variation. This serves as the reference target for evaluating discretization artifacts in the phased-array synthesis.

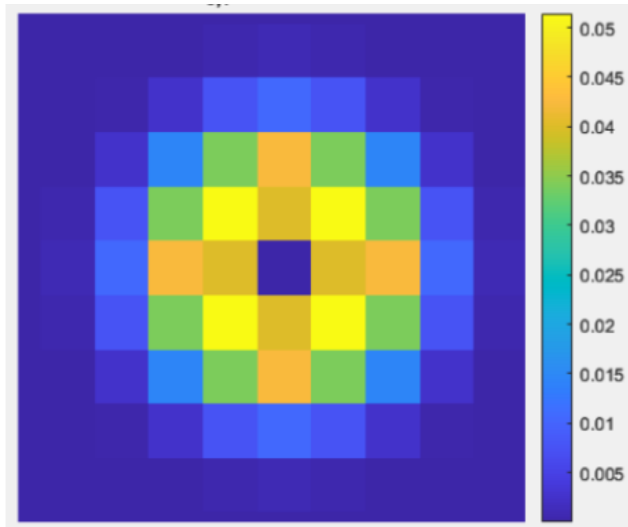

Figure 1: Normalized far-field intensity of the ideal $LG_{0,1}$ mode.

Figure 2 shows the far-field intensity synthesized by the seven-site hexagonal geometry with phases $\phi_k = \theta_k$ on the outer ring and the central site disabled ($A_{\text{center}} = 0$). The synthesized pattern reproduces the two defining qualitative features of the target OAM beam: (i) a clear central null and (ii) an annular maximum at approximately the same radius as the ideal case. The main visible deviation is a weak six-fold azimuthal modulation around the ring accompanied by faint sidelobes. Physically, these features are expected when a continuous 2π azimuthal phase ramp is represented by only six discrete phase samples and a finite set of displaced Gaussian emitters.

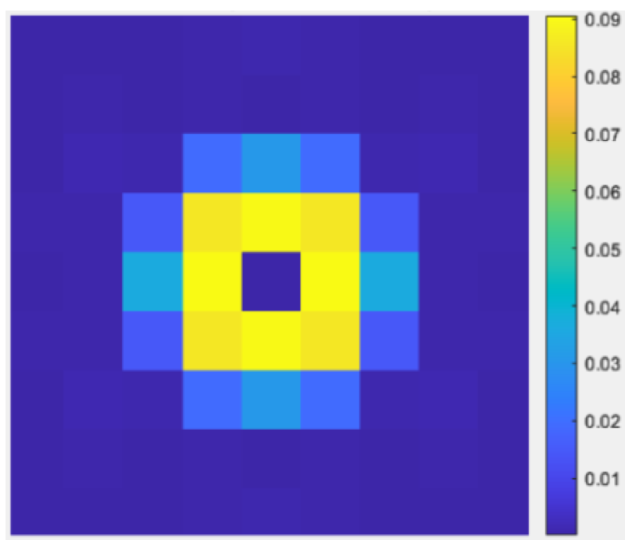

Figure 2: Far-field intensity of the hexagonal phased array (center disabled).

To localize the mismatch, Figure 3 plots the point-by-point intensity difference between the normalized array and ideal far-field patterns. The dominant discrepancies lie on and near the main annulus, where the discretized pattern alternates between slight overestimation and underestimation at different azimuthal angles, consistent with the observed six-fold symmetry. Additional weaker differences appear outside the annulus, corresponding to sidelobes introduced by the finite beamlet spacing and the Gaussian beamlet envelopes. Quantitatively, the mean-squared error between the normalized far-field intensity maps is

$$\mathrm{MSE}_{\mathrm{far}} \approx 7.29 \times 10^{-8},$$

while the near-field MSE between $I_{\mathrm{array}}(x, y)$ and $I_{\mathrm{LG}}(x, y)$ is

$$\mathrm{MSE}_{\mathrm{near}} \approx 5.6 \times 10^{-11}.$$

Because the far field emphasizes spatial-frequency content, it is more sensitive to discretization than the near-field intensity at the waist. (Since MSE is computed between power-normalized maps on a finite grid/window, its absolute value is mainly meaningful for comparisons within this modeling framework rather than as a direct match to the metric definition used in [1].)

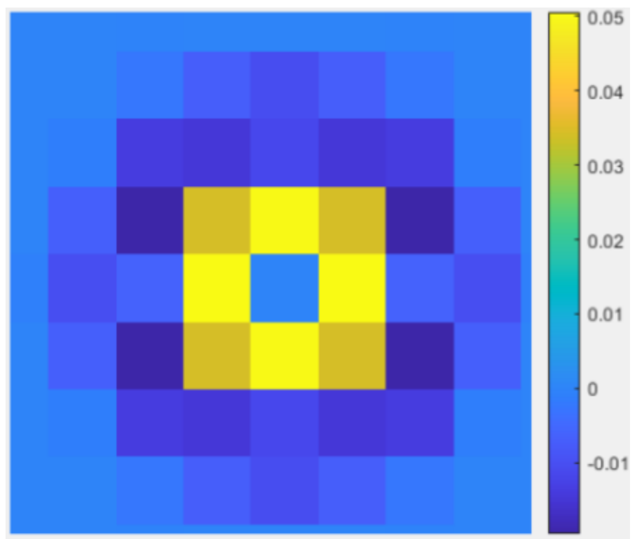

Figure 3: Far-field intensity difference between the array and ideal $\mathrm{LG}_{0,1}$.

Intensity-only comparisons do not fully capture structured-light fidelity because OAM modes are defined by their complex field. To quantify mode purity, I therefore compute the complex-field mode-overlap fidelity

$$F = \frac{\left|\sum_j \tilde{E}^*_{\mathrm{array},j}\, \tilde{E}_{\mathrm{LG},j}\right|^2}{\left(\sum_j |\tilde{E}_{\mathrm{array},j}|^2\right)\left(\sum_j |\tilde{E}_{\mathrm{LG},j}|^2\right)}, \tag{11}$$

where j indexes pixels in the discretized far-field plane. For the parameters used here, $F \approx 0.71$, indicating that most of the synthesized field power lies in the desired $\mathrm{LG}_{0,1}$-like component, with the remainder distributed into other spatial modes associated with discretization (e.g., six-fold symmetry components and sidelobes).

Figure 4 provides a complementary 1D comparison via a horizontal cross-section through the far-field center. Both curves peak at nearly the same radial coordinate, confirming that the chosen ring radius R reproduces the target donut radius. The residual oscillations in the array profile provide a compact signature of discretization-induced azimuthal modulation.

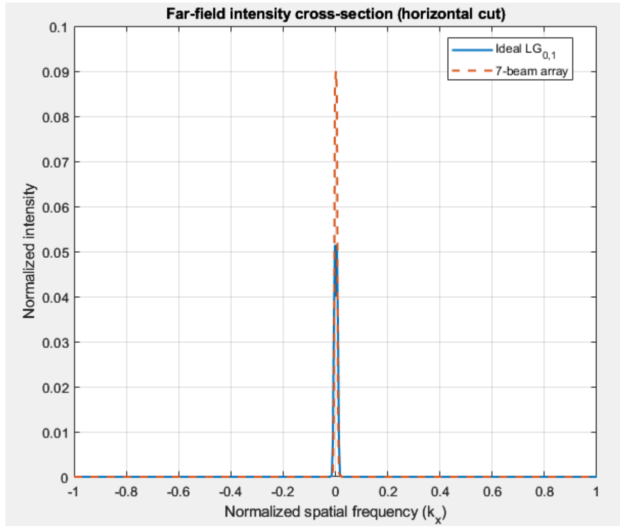

Figure 4: Normalized horizontal far-field cross-section of ideal $LG_{0,1}$ vs. array (center disabled).

Overall, the simulations support the key message in [1]: even modest channel counts can generate OAM-like donut beams, but limited angular sampling of the phase front introduces symmetry-locked artifacts. In this simplified model, the primary levers for improved mode purity are increasing channel count (denser phase sampling), choosing R to maintain strong beamlet overlap, and tuning the beamlet waist w_b to balance overlap against excessive smoothing.

Conclusions

In this review, I used standard Gaussian and Laguerre–Gaussian beam theory [2] to analyze how well a discretized hexagonal phased array can reproduce an ideal $LG_{0,1}$ OAM beam, motivated by Lemons et al. [1]. Numerical simulations in MATLAB show that the array successfully generates a donut-shaped far-field pattern with a central null, capturing the main qualitative features of the $LG_{0,1}$ mode.

At the same time, a quantitative comparison using mean-squared error metrics and a complex-field mode-overlap fidelity reveals azimuthal modulation and side lobes associated with the finite number of beamlets and their hexagonal arrangement. For the specific parameters used here, the far-field overlap $F \approx 0.71$ indicates that most of the power resides in the desired first-order OAM-like mode, but a non-negligible fraction is spread into higher-order or non-ideal components. These findings are consistent with the trends reported by Lemons et al. for larger channel counts and illustrate the trade-off between system complexity and structured-light fidelity.

References

[1] R. Lemons, W. Liu, J. C. Frisch, A. Fry, J. Robinson, S. R. Smith, and S. Carbajo, "Integrated structured light architectures," *Scientific Reports*, vol. 11, no. 796, pp. 1–8, 2021.

[2] J.-M. Liu, *Principles of Photonics*. Cambridge, U.K.: Cambridge University Press, 2016.

[3] D. L. Andrews, *Structured Light and Its Applications: An Introduction to Phase-Structured Beams and Nanoscale Optical Forces*. Amsterdam, The Netherlands: Academic Press, 2011.

Code Appendix

MATLAB Code for Method Section

```
fx >> %% Parameters and grid
Nx = 512;                % number of points in x
Ny = 512;                % number of points in y
L  = 4e-3;               % physical size of simulation window [m] (arbitrary scale)

x = linspace(-L/2, L/2, Nx);
y = linspace(-L/2, L/2, Ny);
[XX, YY] = meshgrid(x, y);

Rho   = sqrt(XX.^2 + YY.^2);   % radius in waist plane
Theta = atan2(YY, XX);         % azimuthal angle

%% Ideal LG_0,1 beam (p = 0, l = 1)
w0 = 0.6e-3;   % waist of ideal LG beam

% field envelope (normalization constant C is irrelevant after normalization)
E_LG = (sqrt(2).*Rho./w0) .* exp(-(Rho.^2)./w0.^2) .* exp(1i*Theta);
I_LG = abs(E_LG).^2;
I_LG = I_LG / sum(I_LG(:));    % normalize total power to 1

%% 7-beam hexagonal phased array
wb    = 0.5e-3;   % waist of each beamlet
Rring = 0.8e-3;   % radius of hexagonal ring

E_array = zeros(size(XX));

% central beam (set A0 = 0 for an OAM-like donut)
A0 = 0;
E_array = E_array + A0 * exp(-(XX.^2 + YY.^2)/wb^2);

% six outer beams
for k = 1:6
    theta_k = 2*pi*(k-1)/6;    % angular position
    xk = Rring * cos(theta_k);
    yk = Rring * sin(theta_k);
    phi_k = theta_k;           % 2*pi phase ramp around ring

    E_k = exp(-((XX-xk).^2 + (YY-yk).^2)/wb^2) .* exp(1i*phi_k);
    E_array = E_array + E_k;
end

I_array = abs(E_array).^2;
I_array = I_array / sum(I_array(:));    % normalize total power to 1

%% Far-field approximation via FFT
E_LG_FF    = fftshift(fft2(E_LG));
E_array_FF = fftshift(fft2(E_array));

I_LG_FF    = abs(E_LG_FF).^2;
I_array_FF = abs(E_array_FF).^2;

% normalize far-field intensities
I_LG_FF    = I_LG_FF    / sum(I_LG_FF(:));
I_array_FF = I_array_FF / sum(I_array_FF(:));

%% Mode-overlap fidelity F (far field, complex fields)
E_LG_vec    = E_LG_FF(:);
E_array_vec = E_array_FF(:);

num = abs(sum(conj(E_array_vec) .* E_LG_vec)).^2;
den = sum(abs(E_array_vec).^2) * sum(abs(E_LG_vec).^2); ...
```

```matlab
num = abs(sum(conj(E_array_vec) .* E_LG_vec)).^2;
den = sum(abs(E_array_vec).^2) * sum(abs(E_LG_vec).^2);
F   = num / den;

%% Mean-squared error (near field and far field)
MSE_near = mean((I_array(:)    - I_LG(:)   ).^2);
MSE_far  = mean((I_array_FF(:) - I_LG_FF(:)).^2);

fprintf('MSE (near field): %g\n', MSE_near);
fprintf('MSE (far field):  %g\n', MSE_far);
fprintf('Mode overlap F (far field): %g\n', F);

%% FIGURE 1: Ideal LG_0,1 far-field intensity
figure;
imagesc(I_LG_FF);
axis image off;
title('Ideal LG_{0,1} Far-Field Intensity');
colorbar;

%% FIGURE 2: 7-beam array far-field intensity
figure;
imagesc(I_array_FF);
axis image off;
title('7-Beam Array Far-Field Intensity');
colorbar;

%% FIGURE 3: Difference map (array - ideal)
figure;
imagesc(I_array_FF - I_LG_FF);
axis image off;
title('Difference: Array - Ideal LG_{0,1}');
colorbar;

%% FIGURE 4: Horizontal cross-section comparison
mid = round(Ny/2);                % index of horizontal center line
kx_norm = linspace(-1, 1, Nx);    % normalized spatial-frequency axis

figure;
plot(kx_norm, I_LG_FF(mid,:), 'LineWidth', 1.5);
hold on;
plot(kx_norm, I_array_FF(mid,:), '--', 'LineWidth', 1.5);
xlabel('Normalized spatial frequency (k_x)');
ylabel('Normalized intensity');
legend('Ideal LG_{0,1}', '7-beam array', 'Location', 'Best');
title('Far-field intensity cross-section (horizontal cut)');
grid on;
```